Two-Qubit Engine Fueled by Entanglement and Local Measurements

Léa Bresque, Patrice A. Camati, Spencer Rogers, Kater Murch, Andrew N. Jordan, and Alexia Auffèves

A two-qubit engine fueled by entanglement and local measurements

Léa Bresque,[1] Patrice A. Camati,[1] Spencer Rogers,[2] Kater Murch,[3] Andrew N. Jordan,[2,4] and Alexia Auffèves[1]

[1]*Université Grenoble Alpes, CNRS, Grenoble INP, Institut Néel, 38000 Grenoble, France*
[2]*Department of Physics and Astronomy, University of Rochester, Rochester, NY 14627, USA*
[3]*Department of Physics, Washington University, St. Louis, Missouri 63130*
[4]*Institute for Quantum Studies, Chapman University, Orange, CA, 92866, USA*

We introduce a two-qubit engine that is powered by entanglement and local measurements. Energy is extracted from the detuned qubits coherently exchanging a single excitation. Generalizing to an N-qubit chain, we show that the low energy of the first qubit can be up-converted to an arbitrarily high energy at the last qubit by successive neighbor swap operations and local measurements. We finally model the local measurement as the entanglement of a qubit with a meter, and we identify the fuel as the energetic cost to erase the correlations between the qubits. Our findings extend measurement-powered engines to composite working substances, and provide a microscopic interpretation of the fueling mechanism.

Understanding quantum measurements from a thermodynamic standpoint is one of the grand challenges of quantum thermodynamics, with strong fundamental and practical implications in various fields ranging from quantum foundations to quantum computing. Quantum measurement has a double status: on one hand, it is the process that allows the extraction of information from a quantum system. In the spirit of classical information thermodynamics, its "work cost" was thus quantitatively analyzed as the energetic toll to create correlations between the system and a memory [1–3]. On the other hand, as stochastic processes, quantum measurements also lead to wavefunction collapse. Measurements can thus behave as a source of entropy and energy, playing a role similar to a bath. The energetic fluctuations generated by a classical measuring device have recently been exploited as a new kind of fuel in so-called measurement-driven engines [4–9], and quantum fridges [10–12].

Another core concept, quantum entanglement [13], was identified by Schrödinger as *the* characteristic trait of quantum physics. This feature of quantum mechanics was identified by Einstein, Podolsky, and Rosen [14] in their attempt to show quantum mechanics was incomplete and later derided by Einstein as "spooky action at a distance". It has come to be viewed as an essential resource in various quantum technologies. The spooky action is the consequence of wavefunction collapse, which happens because the measured non-local state is not an eigenstate of the local measured observable. Moreover, entanglement is crucial to model the first step of a measurement process, the so-called "pre-measurement" introduced by Von Neumann [15]. In this Letter, we exploit these features to design a new generation of quantum measurement powered engines, while deepening our understanding of measurement as fuel.

We first propose a bipartite engine made of two detuned qubits, that become entangled through the coherent exchange of a quantum of excitation. When the red-detuned qubit, A, is initially excited, the excitation is partially transferred to the blue-detuned qubit, B. While the qubits are still coupled, local energy measurements can then project the excitation into B with a finite probability, resulting in some net energy gain [16]. We provide evidence that the energy gain comes from
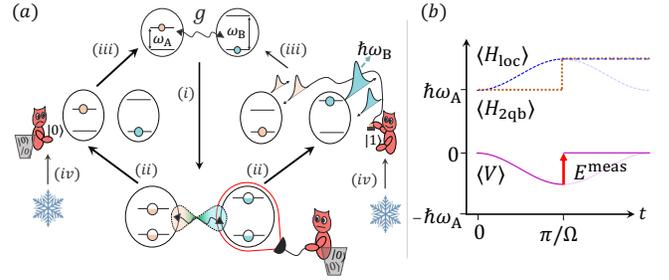
FIG. 1. A two-qubit engine. (a) Scheme of the engine cycle. *(i)* Starting from $|10\rangle$, the qubits get entangled by coherently exchanging an excitation. *(ii)* A demon performs an energy measurement on qubit B at $t_0 = \pi/\Omega$. *(iii)* Feedback. If B is found in the excited state, a π pulse is applied to each qubit. The energy of B is extracted and A is re-excited. If not, nothing is done. At the end of this step, the qubits are back to their initial state. *(iv)* Reset of the demon's memory. (b) Evolution of $\langle H_{2qb}\rangle$ (dotted brown), $\langle H_{loc}\rangle$ (dashed blue), and $\langle V\rangle$ (solid magenta) as a function of time (See text).

the measurement channel, and corresponds to the cost of erasing the quantum correlations between the qubits. This contrasts with former entanglement engines powered with thermal resources [17–20]. Exploiting the information carried by the measurement allows work extraction, in a cycle similar to the classical Szilard engine [21] or its quantum generalization [22]. Frequency up-conversion is obtained by extending the protocol to an N-qubit chain.

We go on to investigate the quantum origin of the fueling mechanism by modeling the pre-measurement step. As one of the qubits gets entangled with a quantum meter, energy flows from the qubit-qubit correlations into the qubits-meter correlations. We demonstrate that the measurement fuel introduced in the first part corresponds to the energy needed to couple and decouple the quantum meter, i.e. to the work cost of operating the measurement channel. By providing new insights into the physics of measurement fueling, our findings shed new light on the double nature of quantum measurement, both a cost and a resource.

An entangled-qubits engine—The basic mechanism of our

engine is illustrated in Figs. 1(a) and 1(b). It involves two qubits A and B of respective transition frequencies ω_A and ω_B, whose evolution is ruled by the Hamiltonian

$$H_{2\text{qb}} = \sum_{i=A,B} \hbar\omega_i \sigma_i^\dagger \sigma_i + \hbar\frac{g(t)}{2}(\sigma_A^\dagger \sigma_B + \sigma_B^\dagger \sigma_A). \quad (1)$$

We have introduced the lowering operator $\sigma_i = |0_i\rangle\langle 1_i|$ for the qubit $i \in \{A, B\}$. The first term of $H_{2\text{qb}}$ is the free Hamiltonian of the qubits. It thus features "local" one-body terms that we shall denote as H_{loc}. The second term, which we denote by V, couples the qubits, giving rise to entangled states. The coupling channel can be switched on and off, which is modeled by the time-dependent coupling strength $g(t)$. In the rest of the paper we consider a positive detuning $\delta = \omega_B - \omega_A$. For simplicity, we denote the product states $|x_A\rangle \otimes |y_B\rangle$ as $|xy\rangle$, where $x, y \in \{0, 1\}$.

The engine cycle encompasses four steps: (i) *Entangling evolution.* At time $t = 0$, the qubits are prepared in the state $|\psi_0\rangle = |10\rangle$ of mean energy $\langle H_{2\text{qb}}\rangle = \langle\psi_0| H_{2\text{qb}} |\psi_0\rangle = \hbar\omega_A$. The coupling term is switched on with a strength g. Since $|\psi_0\rangle$ is a product state, its mean energy does not change during this switching process, which is thus performed at no cost. The qubits' state then evolves into an entangled state $|\psi(t)\rangle$ where the initial excitation gets periodically exchanged between the two qubits, with

$$|\psi(t)\rangle = (c_\theta^2 e^{i\Omega t/2} + s_\theta^2 e^{-i\Omega t/2}) |10\rangle$$
$$- c_\theta s_\theta (e^{i\Omega t/2} - e^{-i\Omega t/2}) |01\rangle. \quad (2)$$

We have defined $c_\theta = \cos(\theta/2)$, $s_\theta = \sin(\theta/2)$, θ as $\tan(\theta) = g/\delta$, and $\Omega = \sqrt{g^2 + \delta^2}$ the generalized Rabi frequency that characterizes the periodic energy exchange.

$\langle H_{\text{loc}}\rangle(t)$ and $\langle V\rangle(t)$ are plotted on Fig. 1(c). As expected from unitary evolution, their sum remains constant and equal to its initial value $\hbar\omega_A$. The periodic exchange of the single excitation between A and B gives rise to oscillations of the local energy component. This evolution is compensated by the opposite oscillations of the coupling energy $\langle V\rangle(t) \leq 0$. This term appears here as a binding energy of purely quantum origin, whose presence ensures that the total energy and the number of excitations are both conserved.

(ii) *Measurement.* $\langle H_{\text{loc}}\rangle$ and $|\langle V\rangle(t)|$ reach a maximum when $t_0 = \pi/\Omega$ where $|\psi(t_0)\rangle = i[\cos(\theta) |10\rangle - \sin(\theta) |01\rangle]$. At this time, a local projective energy measurement is performed on qubit B, and its outcome is encoded in a classical memory M. Here we consider an instantaneous process, performed with a classical measuring device. A more elaborate model of the measurement will be presented in the last part of the paper. In turn, the average qubits' state becomes a statistical mixture $\rho(\theta) = \cos^2(\theta) |10\rangle\langle 10| + \sin^2(\theta) |01\rangle\langle 01|$, erasing the quantum correlations between them and thus bringing the binding energy $\langle V(t_0)\rangle$ to zero. The average energy input reads

$$E^{\text{meas}} = -\langle V(t_0)\rangle = \Delta\langle H_{2\text{qb}}\rangle = \hbar\delta\sin^2(\theta) \geq 0, \quad (3)$$

where $\Delta\langle\cdot\rangle$ features the change of mean energy. Conversely, the von Neumann entropy of the qubits increases by an amount $S^{\text{meas}} = -\text{Tr}[\rho(\theta)\log_2(\rho(\theta))]$, that reads

$$S^{\text{meas}} = -\cos^2(\theta)\log_2[\cos^2(\theta)] - \sin^2(\theta)\log_2[\sin^2(\theta)]. \quad (4)$$

We use $\log_2$, such that all entropies are expressed in bits. The simultaneous energy and entropy increases signal that the qubits are being fueled; the ratio $\mathcal{T}^{\text{meas}} = E^{\text{meas}}/S^{\text{meas}}$ characterizes the fueling process. $\mathcal{T}^{\text{meas}}$ diverges in the limit of large coupling and small detuning ($\theta \to \pi/2$), i.e. the measurement can input a finite amount of energy with vanishing entropy. This contrasts with isothermal processes, where energy and entropy inputs are related by the bath temperature. Note that the fueling step solely involves the qubits characteristics. It does not fully describe the measurement process, which also involves the creation of classical correlations between the qubits and the classical memory in the basis $\{|10\rangle, |01\rangle\}$, quantified by their mutual information $I^{\text{meas}}(S : M)$ (See Suppl.[24]). For ideal measurements $I^{\text{meas}}(S : M) = S^{\text{meas}}$.

(iii) *Feedback.* The information stored in the memory is now processed to convert the fuel into work. To do so, the coupling term is switched off at time t_0^+. Since the quantum correlations between the qubits have been erased, the switching-off is implemented at no energetic cost. If the excitation is measured in B, which happens with probability $P_{\text{succ}}(\theta) = \sin^2(\theta)$, both A and B undergo a resonant π pulse, such that B emits a photon while A absorbs one. The work $W = \hbar\delta$ is extracted and the qubits are reset to their initial state $|10\rangle$. Conversely if the excitation is measured in A, no pulse is implemented and the cycle restarts. Eventually, the mean work extracted is $W = E^{\text{meas}}$. At the end of this feedback step, the qubits' entropy vanishes, and a maximal amount of mutual information $|\Delta I(S : M)| = I^{\text{meas}}(S : M)$ is consumed.

(iv) *Erasure.* The memory is erased in a cold bath, which costs a minimal work proportional to S^{meas} [23].

The quantum engine described above extends the concept of measurement-powered engines, originally proposed for single parties as working substances [4–8], to entangled systems. In those proposals the engine is fueled by quantum measurement back-action, which can only take place when the measured system state has coherences in the basis of the measured observable. Both quantum measurement and coherence thus contribute to the fueling process. Similarly, in the present bipartite engine, both local measurements and entanglement are necessary for work extraction.

Measurement energy vs information as fuel—The engine proposed above exploits two complementary features of quantum measurements: on the one hand, they bring energy and entropy, on the other hand, they extract information that can be further used to convert the energy input into work. Now focusing on the measurement and feedback steps, we analyze these energetic and informational resources, and how they respectively impact the performance of the bipartite engine.
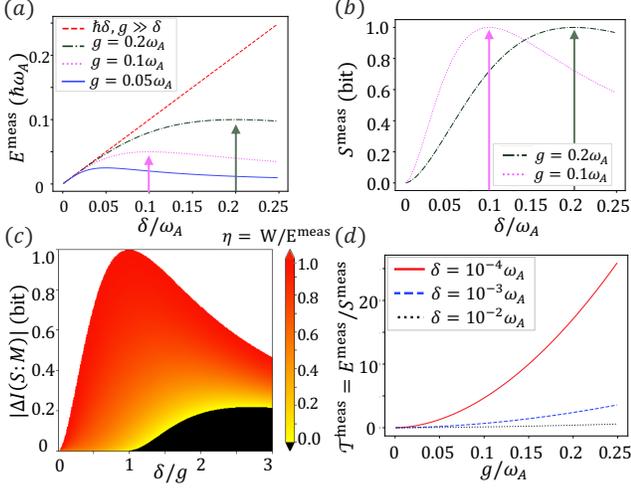
FIG. 2. Measurement energy vs information as fuel. (a) Energy E^{meas} and (b) entropy S^{meas} inputs as a function of the detuning δ, for various coupling strengths g. (c) Work extraction ratio $\eta = W/E^{\text{meas}}$ (color scale) as a function of δ/g and consumed mutual information $|\Delta I(S : M)|$. The black region corresponds to $\eta = 0$. d) Yield of information to work conversion $\mathcal{T}^{\text{meas}}$ as a function of g for various δ.

The mean energy E^{meas} and entropy S^{meas} input by the measurement process are plotted in Figs. 2(a) and 2(b) as a function of the detuning δ, for various coupling strengths g. As indicated in the figure, they are both maximized for $\delta = g$. Converting the measurement energy into work requires the processing of this information during the feedback step. The conversion is optimal ($W = E^{\text{meas}}$) when all information is consumed, which corresponds to the ideal cycle presented above. Non-optimal work extraction results from an incomplete consumption of information, $|\Delta I(S : M)| < I^{\text{meas}}(S : M)$, yielding a conversion ratio $\eta = W/E^{\text{meas}} < 1$. We have modeled such an imperfect feedback, see Suppl. [24]. Figure 2(c) features η as a function of δ/g and $\Delta I(S : M)$, clearly showing the work value of information—the larger the consumed information, the larger the conversion ratio. Interestingly, the figure reveals that work can be extracted even if $\Delta I(S : M) = 0$. This is the case when $P_{\text{succ}}(\theta) > 1/2$, which happens when $\delta/g < 1$. Then the π-pulses can be blindly applied, still leading to a net work extraction $W = \hbar\delta[\sin^2(\theta) - \cos^2(\theta)]$. This mechanism solely exploits the energy input by the measurement, but not the extracted information; it is at play, e.g. in single temperature engines [6, 7]. By contrast, information processing is necessary when $\delta \geq g$. Note that in all non-ideal cases where information is not fully consumed, an additional step must be included in the cycle, to reset the qubits' state.

From now on we suppose the feedback to be perfect, such that the net work extracted is $W = E^{\text{meas}}$, and conversely, $S^{\text{meas}} = |\Delta I(S : M)|$. Therefore $W = \mathcal{T}^{\text{meas}}|\Delta I(S : M)|$. Interestingly, now $\mathcal{T}^{\text{meas}}$ is a measure of efficiency of information-to-work conversion. Such efficiency is usually bounded by the bath temperature in Maxwell's demons,

that are fueled by a thermal bath [1, 25]. $\mathcal{T}^{\text{meas}}$ is plotted on Fig. 2(d) as a function of g for various values of the detuning δ. As it appears on the figure, it is not bounded and increases as a function of g. This reveals that in the limit $g \gg \delta$, a finite amount of work can be extracted by processing a vanishingly small amount of information. This effect is similar to the Zeno regime [4, 26], where work extraction relies on measurements whose outcomes are nearly deterministic.
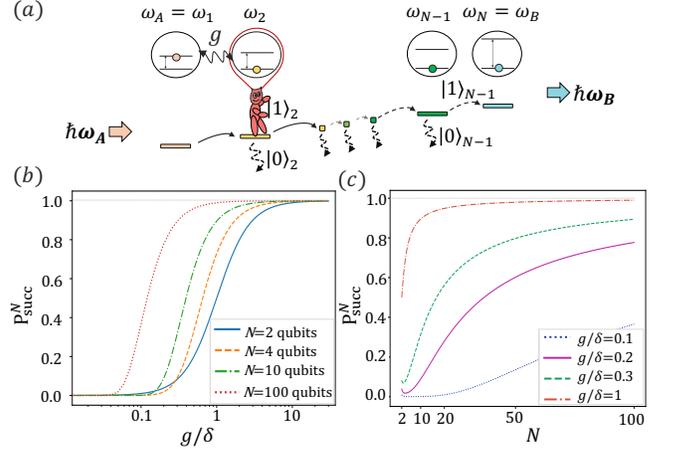
FIG. 3. Entanglement and measurement based up-conversion mechanism. (a) Scheme of the frequency up-converter (See text). Probability of transfer P_{succ}^N as a function of g/δ for various N (b) and as a function of N for various g/δ (c). The grey lines indicate constant values as guides to the eye.

Up-conversion—We propose to realize energy up-conversion, by extending the fueling mechanism to a chain of N qubits of increasing frequency as depicted in Fig. 3(a) . We denote the frequency of the qubit i by $\omega_i = \omega_A + (i - 1)\delta/(N - 1)$, with $i \in \{1, 2, ..., N\}$ with $\delta = \omega_B - \omega_A$. At time $t = 0$, the qubit 1 is excited and the coupling g between qubit 1 and qubit 2 is switched on, its Rabi frequency being $\Omega_N = \sqrt{g^2 + (\delta/(N - 1))^2}$. At time $t_N = \pi/\Omega_N$, the energy of qubit 2 is measured. The process stops if it is found in the ground state, which happens with probability $\cos^2(\theta_N)$, where $\tan(\theta_N) = (N - 1)g/\delta = (N - 1)\tan(\theta)$. If the excitation is successfully transferred to qubit 2, the coupling between 1 and 2 is switched off and the coupling between 2 and 3 is switched on. The same process is repeated between qubits k and $k + 1$ until the excitation gets detected in qubit N, which happens with probability $P_{\text{succ}}^N = \sin^{2(N-1)}(\theta_N)$. P_{succ}^N is plotted in Fig. 3(b) and 3(c) as a function of g/δ and N. For fixed values of g and δ, it is clearly advantageous to increase the number of intermediate qubits. The mechanism at play is reminiscent of the quantum Zeno effect. An analytic demonstration is presented in the Suppl. [24].

Origin of the measurement fuel—In all measurement pow-

ered engines proposed until now, the measuring device was taken as classical and the fuel identified with the energetic counterpart of the measurement postulate. We now investigate the quantum origin of the fuel. As described above, the fueling step solely involves the qubits mean energy and entropy – not the classical information about their state. From the measured system perspective, it can thus be safely modeled by Von Neumann's pre-measurement step [15]. Namely, the measured system gets entangled with a quantum meter, which erases its quantum coherences in the basis of the measured observable and increases its reduced entropy. In the rest of this paper, we focus on the energetic flows taking place during this pre-measurement.

The pre-measurement takes place between $t = t_0$ and t_m while the qubits are still coupled, as depicted in Fig. 4(a). It involves a third qubit m with degenerate energy levels $|0_m\rangle$ and $|1_m\rangle$ as our quantum meter, that can be coupled to the qubit B through the Hamiltonian:

$$V_m(t) = \hbar\chi(t)\sigma_B^\dagger\sigma_B \otimes \sigma_x^m. \tag{5}$$

$\chi(t)$ is the coupling strength, with $\chi(t) = \chi$ for $t = [t_0, t_m]$ and 0 otherwise. We choose $\chi \gg g$, to ensure the process takes place on small time-scales with respect to the Rabi period. This defines the parameter $\epsilon = g/\chi$. Importantly, ϵ is small but finite since the measurement is implemented on still-interacting qubits.

At t_0^-, the meter m is prepared in $|0_m\rangle$. A and B are in the entangled state $|\psi(t_0)\rangle$, such that the global state reads $|\Psi(t_0)\rangle = i(\cos(\theta)|100_m\rangle - \sin(\theta)|010_m\rangle)$. Since $\langle V_m(t_0)\rangle = 0$, the pre-measurement channel is switched on at no energy cost. The joint qubits-meter system then evolves under the total Hamiltonian $H = H^{(0)} + H^{(1)}$, where $H^{(0)} = H_{loc} + V_m$ (resp. $H^{(1)} = V$) rules the evolution at zeroth order (resp. at first order) in the small parameter ϵ. The dynamics is solved at first order in [24], yielding $|\Psi^{(1)}(t)\rangle = |\Psi^{(0)}(t)\rangle + |\delta\Psi(t)\rangle$ where $|\delta\Psi(t)\rangle$ is of order ϵ. The computed populations are plotted on Fig. 4(b). The evolution, to lowest order in ϵ, features a quantum non-demolition pre-measurement [27, 28]: the state $|10\rangle$ (resp. $|01\rangle$) is preserved by the evolution and gets correlated with $|0_m\rangle$ (resp. $|1_m\rangle$). The qubits-meter quantum correlations are maximal when $t_m = t_0 + \pi/\chi$, where the global state reads $|\Psi^{(0)}(t_m)\rangle = i[\cos(\theta)|100_m\rangle - \sin(\theta)|011_m\rangle]$. At this time the reduced qubits state bears no coherence in the $\{|01\rangle, |10\rangle\}$ basis, signaling that the pre-measurement is completed.

We now focus on the energy flows during the pre-measurement. While Fig.1(b) pictures the instantaneous limit of the process $g/\chi \ll 1$ for the qubits only, the evolution of the qubits and meter mean energy components is plotted in Fig. 4(c) up to first order in ϵ. Since the pre-measurement is a unitary process, the total qubits-meter energy is conserved, yielding at any time $\langle H_{loc}\rangle + \langle V\rangle + \langle V_m\rangle = \hbar\omega_A$. We first consider the reduced qubits energy $\langle H_{2qb}\rangle = \langle H_{loc}\rangle + \langle V\rangle$. Perturbative calculations show that $\langle H_{loc}\rangle$ (resp. $\langle V\rangle$) remain constant up to first order in ϵ (resp. at zeroth or-
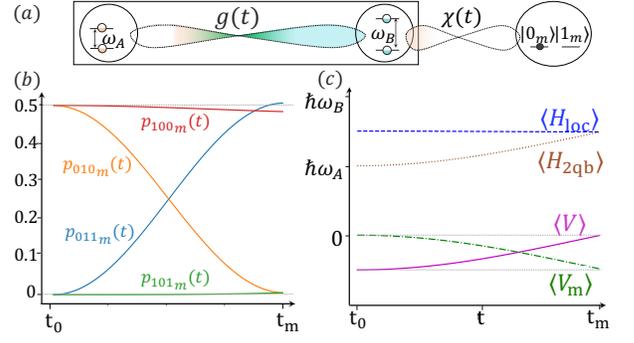
FIG. 4. Energetics of the pre-measurement step. (a) Local quantum measurement of qubit B allows for the creation of correlations between the meter m and the AB system and destroys correlations between the qubits. (b) Full state decomposition in the $\{|100_m\rangle, |101_m\rangle, |010_m\rangle, |011_m\rangle\}$ basis during the pre-measurement step. (c) Expectation values of $\langle H_{2qb}\rangle = \langle H_{loc}\rangle + \langle V\rangle$, $\langle H_{loc}\rangle$, $\langle V_m\rangle$, and $\langle V\rangle$ as a function of the pre-measurement time $t \in [t_0, t_m]$. The curves in the figure are calculated for $\chi = 10\Omega$ and $g = \delta$. The grey lines indicate constant values as guides to the eye.

der) [24]. $\langle H_{2qb}\rangle$ thus follows the first order contribution of the qubits binding energy $\langle V^{(1)}\rangle = \langle\Psi^{(0)}(t)|V|\Psi^{(0)}(t)\rangle$, whose absolute value scales like the qubits' coherences in the $\{|01\rangle, |10\rangle\}$ basis. Therefore, $\langle H_{2qb}\rangle$ increases until the pre-measurement is completed and $\langle H_{2qb}\rangle = \langle H_{loc}\rangle$, yielding the energy input $E^{meas} = |\langle V(t_0)\rangle|$ defined above.

Energy conservation requires the qubits energy increase to be compensated by an equivalent decrease of the qubits-meter coupling, until time t_m where $\langle V_m^{(1)}(t_m)\rangle = \langle V(t_0)\rangle$. Note this is a first order effect, $\langle V_m^{(0)}\rangle = \langle\psi^{(0)}|V_m|\psi^{(0)}\rangle$ being constantly null. However since V_m scales as χ, $\langle V_m^{(1)}(t_m)\rangle$ remains finite and of order g even in the instantaneous limit $g/\chi \ll 1$. Our calculation reveals the direction of the energy flow during the pre-measurement process: The binding energy initially localized between the qubits is transferred between the qubits and the meter. Finally, the qubits-meter coupling must switched off before any further manipulation on the qubits can be made. The work cost to operate the pre-measurement channel equals $\langle -V_m^{(1)}(t_m)\rangle = E^{meas}$, thus corresponds to the measurement fuel introduced in the first part of the paper. Note that converting the fuel into work as presented above would require to extract the information on the qubits state, by performing a final projective measurement on the quantum meter. In the absence of the qubits-meter coupling term, such operation has no impact on the qubits energy.

Outlook—Our findings advance quantum measurement engines to encompass quantum entanglement and energy correlations, showing how entanglement engines may be powered by quantum measurement. From a conceptual standpoint, they shed new light on the measurement-based fueling process, and provide a unified view on former analyses based on analogies

with work and heat exchanges. It should be recalled however that the concepts of work and heat were historically defined with respect to thermal noise and resources. Our results, on the other hand, are solely based on a stochasticity of quantum nature [29]. They contribute to the emergence of a new framework—"Quantum Energetics"—where thermodynamic concepts will be relevant in the presence of any kind of noise, especially at zero temperature where most quantum technology tasks are envisioned [30].

In the future, it will be interesting to study the autonomous regimes of our engine where measurement and dissipation become time-independent processes, leading to the design of engines exploiting decoherence as a resource. This would bridge the gap with the field of dissipation engineering [31, 32], where dissipation is harnessed to produce nontrivial quantum states and desirable quantum dynamics. Such reservoir engineering has been recently employed in the circuit-QED architecture [33–36]—the same experimental platform on which we expect to realize our proposed engine.

[1] J. Parrondo, J. Horowitz, and T. Sagawa, Nature Phys 11, 131 (2015).

[2] T. Sagawa and M. Ueda, Phys. Rev. Lett. 102, 250602 (2009).

[3] K. Jacobs, Phys. Rev. E 86, 040106(R) (2012).

[4] C. Elouard, D. Herrera-Martí, B. Huard, and A. Auffèves, Phys. Rev. Lett 118, 260603 (2017).

[5] C. Elouard and A. N. Jordan, Phys. Rev. Lett. 120, 260601 (2018).

[6] J. Yi, P. Talkner, and Y. W. Kim, Phys. Rev. E 96, 022108 (2017).

[7] X. Ding, J. Yi, Y. W. Kim, and P. Talkner, Phys. Rev. E 98, 042122 (2018).

[8] A. Jordan, C. Elouard, and A. Auffèves, Quantum Stud.: Math. Found. 61, 203 (2020).

[9] M. H. Mohammady and J. Anders, New J. Phys. 19, 113026 (2017).

[10] M. Campisi, J. Pekola, and R. Fazio, New J. Phys. 19, 053027 (2017).

[11] L. Buffoni, A. Solfanelli, P. Verrucchi, A. Cuccoli, and M. Campisi, Phys. Rev. Lett 122, 070603 (2019).

[12] C. Levy, and A. Kosloff, Phys. Rev. Lett 108, 070604 (2012).

[13] E. Schrödinger, Proceedings of the Cambridge Philosophical Society 31, 555–563 (1935).

[14] A. Einstein, B. Podolsky, and N. Rosen, Phys. Rev. 47, 777 (1935).

[15] J. Von Neumann, Mathematical Foundations of Quantum Mechanics (1955) .

[16] A. N. Jordan and M. Büttiker, Phys. Rev. Lett. 92, 247901 (2004).

[17] A. Tavakoli, G. Haack, N. Brunner, and J. B. Brask, Phys. Rev. A 101, 012315 (2020).

[18] M. Josefsson and M. Leijnse, Phys. Rev. B 101, 081408 (2020).

[19] X. L. Huang, H. Xu, X. Y. Niu, and Y. D. Fu, Phys. Scr. 88, 065008 (2013).

[20] A. Hewgill, A. Ferraro, and G. De Chiara, Phys. Rev. A 98, 042102 (2018).

[21] L. Szilard, Zeitschrift für Physik 53, 840 (1929), [Behav Sci. 9, 301 (1964)].

[22] S. W. Kim, T. Sagawa, S. De Liberato, and M. Ueda, Phys. Rev. Lett. 106, 070401 (2011).

[23] R. Landauer, IBM J. Res. Dev. 5, 183 (1961).

[24] See Supplemental Material at [URL will be inserted by publisher].

[25] Y. Masuyama, K. Funo, Y. Murashita, A. Noguchi, S. Kono, Y. Tabuchi, R. Yamazaki, M. Ueda, and Y. Nakamura, Nat. Comm. 9, 1291 (2018).

[26] C. Erez, D. Gordon, B. Nest, and B. Kurizki, Nature 452, 06873 (2008).

[27] P. Grangier, J. A. Levenson, and J.-P. Poizat, Nature 396, 537 (1998).

[28] Y. Guryanova, N. Friis, and M. Huber, Quantum 4, 222 (2020).

[29] P. Grangier and A. Auffèves, Phil. Trans. R. Soc. A 376, 20170322 (2018).

[30] A. M. Timpanaro, J. P. Santos, and G. T. Landi, Phys. Rev. Lett. 124, 240601 (2020).

[31] J. F. Poyatos, J. I. Cirac, and P. Zoller, Phys. Rev. Lett. 77, 4728 (1996).

[32] E. Kapit, Quantum Science and Technology 2, 033002 (2017).

[33] Y. Liu, S. Shankar, N. Ofek, M. Hatridge, A. Narla, K. M. Sliwa, L. Frunzio, R. J. Schoelkopf, and M. H. Devoret, Phys. Rev. X 6, 011022 (2016).

[34] Y. Lu, S. Chakram, N. Leung, N. Earnest, R. K. Naik, Z. Huang, P. Groszkowski, E. Kapit, J. Koch, and D. I. Schuster, Phys. Rev. Lett. 119, 150502 (2017).

[35] S. Touzard, A. Grimm, Z. Leghtas, S. O. Mundhada, P. Reinhold, C. Axline, M. Reagor, K. Chou, J. Blumoff, K. M. Sliwa, S. Shankar, L. Frunzio, R. J. Schoelkopf, M. Mirrahimi, and M. H. Devoret, Phys. Rev. X 8, 021005 (2018).

[36] R. Ma, B. Saxberg, C. Owens, N. Leung, Y. Lu, J. Simon, and D. I. Schuster, Nature 566, 51 (2019).